Bioresource Technology 133 (2013) 248–255

Contents lists available at SciVerse ScienceDirect

Bioresource Technology

journal homepage: www.elsevier.com/locate/biortech

Biodiesel production by free fatty acid esterification using lanthanum (La^{3+}) and HZSM-5 based catalysts

Sara S. Vieira [a], Zuy M. Magriotis [a,*], Nadiene A.V. Santos [a], Adelir A. Saczk [a], Carla E. Hori [b], Pedro A. Arroyo [c]

[a] Departamento de Química, Universidade Federal de Lavras, 37.200-000 Lavras, MG, Brazil
[b] Faculdade de Engenharia Química, Universidade Federal de Uberlândia, 38.408-144 Uberlândia, MG, Brazil
[c] Departamento de Engenharia Química, Universidade Estadual de Maringá, 87.020-900 Maringá, PR, Brazil

HIGHLIGHTS

- Esterification of fatty acid was studied using lanthanum and HZSM-5 based catalyst.
- Sulfation process caused the formation of strong Brønsted acid sites in the catalysts.
- SLO/HZSM-5 had the lowest deactivation after the third reuse.
- Sulfated catalysts reached close to100% of conversion of oleic acid at 100 °C.
- Sulfated catalysts are new eco-friendly catalyst for the esterification.

GRAPHICAL ABSTRACT

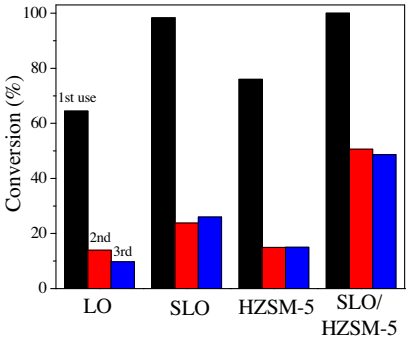

ARTICLE INFO

Article history:
Received 13 September 2012
Received in revised form 15 January 2013
Accepted 17 January 2013
Available online 29 January 2013

Keywords:
Biodiesel
Esterification
Heterogeneous acid catalysts
Lanthanum
HZSM-5

ABSTRACT

In this work the use of the heterogeneous catalysts pure (LO) and sulfated (SLO) lanthanum oxide, pure HZSM-5 and SLO/HZSM-5 (HZSM-5 impregnated with sulfated lanthanum oxide (SO_4^{2-}/La_2O_3)) was evaluated. The structural characterization of the materials (BET) showed that the sulfation process led to a reduction of the SLO and SLO/HZSM-5 surface area values. FTIR showed bands characteristic of the materials and, FTIR-pyridine indicated the presence of strong Brønsted sites on the sulfated material. In the catalytic tests the temperature was the parameter that most influenced the reactions. The best reaction conditions were: 10% catalyst, 100 °C temperature and 1:5 m_{OA}/m_{meOH} for LO, SLO, SLO/HZSM-5 and 10% catalyst, 100 °C temperature and 1:20 m_{OA}/m_{meOH} for HZSM-5. Under these conditions the conversions were: 67% and 96%, for LO and SLO, respectively and 80% and 100%, for HZSM-5 and SLO/HZSM-5, respectively. All catalysts deactivated after the first use, but the deactivation of SLO/HZSM-5 was smaller.

1. Introduction

Energy is a decisive factor for the economic development of a country and the energy crisis increases the urgency of research in this area. In this scenario, biodiesel production stands out, because it is a viable alternative in terms of renewable fuel. Biodiesel is chemically constituted of fatty acid alkyl esters that can be obtained through the transesterification of triglycerides, or from the esterification of fatty acids, both in the presence of a short chain alcohol such as ethanol or methanol and, an acid or base catalyst (Chantras et al., 2011; Encinar et al., 2011; Birla et al., 2012; Yin et al., 2012).

* Corresponding author. Tel.: +55 35 38291889; fax: +55 35 38291812.
E-mail addresses: saraufla@yahoo.com.br (S.S. Vieira), zuy@dqi.ufla.br (Z.M. Magriotis), nadi.ene@hotmail.com (N.A.V. Santos), adelir@dqi.ufla.br (A.A. Saczk), cehori@ufu.br (C.E. Hori), paarroyo@uem.br (P.A. Arroyo).

0960-8524/$ - see front matter © 2013 Elsevier Ltd. All rights reserved.
http://dx.doi.org/10.1016/j.biortech.2013.01.107

The transesterification process is preferable to the esterification due to higher availability of natural raw materials rich in triglycerides, but the esterification process has its importance as an alternative process, because it enables the use of materials rich in free fatty acids present in residues and by-products of industrial biomass processing, mainly the crude oils, acid sludge, frying oils and even products of animal origin such as lard or suet (Marchetti and Errazu, 2008; Semwal et al., 2011; Kim et al., 2012).

The esterification reaction consists of the reaction of a fatty acid with an alcohol in the presence of an acid catalyst. The homogeneous catalysts, usually strong mineral acids, present excellent reaction yields, but they can cause equipment corrosion problems. Thus, the technological challenge for the development of a biodiesel production process by esterification of fatty acids is the development of heterogeneous acid catalysts. These materials should present high activity and stability, easy separation of the products and should not pose corrosion problems to the equipment. These properties would characterize them as environmentally friendly materials (Kirumakki et al., 2006).

Among the several types of heterogeneous catalysts tested for production of biodiesel by esterification reaction, different zeolites can be found: HBEA, HMOR, HZSM-5, HMFI, HFAU and HY (Kirumakki et al., 2006; Aranda et al., 2009; Chung et al., 2008; Chung and Park, 2009; Satyarthi et al., 2011; Selvabala et al., 2011; Costa et al., 2012; Patel and Narkhede, 2012) besides pure and impregnated HBEA with lanthanum ions (La^{3+}) in the transesterification of soybean oil (Shu et al., 2007).

Another promising catalysts for the production of biodiesel through a transesterification/esterification reaction are those based on sulfated metals heterogeneous oxides. Some studies already have proven that the catalytic properties of these solids depend on the starting oxide, the sulfating agent and the thermal treatment employed. Therefore, several studies have been conducted with the objective of generating solids with superacid properties that possess good stability and can be used in various industrial level reactions (Noda et al., 2005).

Among the sulfated oxides already studied as superacid catalysts, zirconium (Furuta et al., 2004; Li et al., 2010; Chang et al., 2012), titanium (Almeida et al., 2008; Li et al., 2010) and tin oxides (Furuta et al., 2004; Lam et al., 2009; Kafuku et al., 2010) stand out. These superacid heterogeneous catalysts can be used in transesterification reactions as well as esterification, for biodiesel production. However, there are still few works reported in the literature that use these superacid solids for such reactions.

Lanthanum oxide has already been studied in catalysis as a support for Ni catalysts in ethanol steam reforming (Fatsikosta et al., 2002); as a catalyst in methane reforming (Cassinelli et al., 2008) and as a catalyst for hydrogen production from steam reforming or oxidative steam reforming of ethanol (Lima et al., 2010). Some studies are using lanthanum oxide as a catalyst for biodiesel production (Yan et al., 2009a,b; Li et al., 2010; Russbueldt and Hoelderich, 2010), but nevertheless, the use of sulfated lanthanum oxide is still unknown in the literature.

Lanthanum and zeolites-based compounds are already known in the literature as highly efficient catalysts for many different acid character reactions such as hydrocarbon isomerization, cracking, alkylation and etherification. However the use of these sulfated catalysts for the production of biodiesel is unknown in the literature.

Based on the above, the objective of this work was to test the heterogeneous catalysts: pure (La_2O_3 – LO) and sulfated (SO_4^{2-}/La_2O_3 – SLO) lanthanum oxide, pure HZSM-5 and HZSM-5 impregnated with sulfated lanthanum oxide SO_4^{2-}/La_2O_3 (forming SO_4^{2-}/La_2O_3/HZSM-5 – SLO/HZSM-5) in esterification reactions for biodiesel production.

2. Methods

2.1. Catalyst preparation

Pure lanthanum oxide (LO – La_2O_3 – Isofar) was used without any treatment to observe if the proposed modifications would cause some effect on its catalytic activity. Sulfated lanthanum oxide (SLO – SO_4^{2-}/La_2O_3) was prepared by impregnation in which 30 g of La_2O_3 were slowly added to 300 mL, 2 mol L^{-1} sulfuric acid solution (Vetec) which was maintained under constant agitation for 3 h at room temperature. The resulting solid was vacuum filtered and dried in an oven at 100 °C for 2 h. The dried material was then calcined in a tube furnace at 400 °C for 3 h under a N_2 flow (150 mL min^{-1}) at a heating rate of 10 °C min^{-1}.

HZSM-5 zeolite used in this study was synthesized at the Department of Chemical Engineering of State University of Maringá, Brazil. Before the reactions it was heated at 120 °C for 24 h to eliminate moisture. For the preparation of SO_4^{2-}/La_2O_3/HZSM-5 (SLO/HZSM-5), 10 g of HZSM-5 and 1 g of La_2O_3 were slowly added to 100 mL of sulfuric acid 2 mol L^{-1} and kept under stirring for 3 h at room temperature. The resulting material was dried and calcined in the same conditions as for preparing the SLO.

2.2. Characterization of catalysts

Thermogravimetric analyses of the catalysts were conducted in a Shimadzu-DTG-60AH thermomechanical analyzer. The experiments were carried out at a heating rate of 10 °C min^{-1}, temperature range 25 °C (room temperature) to 1000 °C, under nitrogen atmosphere. The morphology of the catalysts was obtained by scanning electron microscopy (SEM), using a Leo Evo 40XVP apparatus with a 25 kV tension.

BET (Brunauer–Emmet–Teller) method was used to measure the specific surface area of the catalysts produced, through the physical adsorption of N_2, at different pressures, at 77 K using a Micromeritics model ASAP 2020 analyzer.

FTIR spectra of the materials were recorded on a Digilab Excalibur spectrometer using KBr pellet technique. Each pellet contained exactly 300 mg of KBr and 3 mg of sample.

The catalysts were submitted to the qualitative determination of Brønsted and Lewis acid sites by the infrared spectroscopy technique using pyridine as probe molecule. The samples, in form of self-supported wafers, were heated to 400 °C for 1 h under high vacuum, followed by five air pulses and 30 min of high vacuum. The Lewis and Brønsted acid sites were identified through the analysis of the FTIR spectra of the adsorbed (25 °C) and desorbed (25, 150, 250 and 350 °C for 30 min under high vacuum) pyridine. The analyses were conducted in the Nicolet Magnum 560 equipment.

2.3. Catalytic tests

For the catalytic tests oleic acid (Vetec) was used as a model molecule. The product (methyl oleate) was obtained through the methylic route using 99.9% pure methanol (Cromoline). The experiments were conducted in batch, at different temperatures (50, 75 and 100 °C), catalyst percentages (5%, 10% and 20%), oleic acid/alcohol mass ratios (1:5, 1:10 and 1:20). and residence times (1, 3, 5 and 7 h). The system was sealed and maintained under constant agitation at 300 rpm and, at specific residence times, a 10 μL aliquot was removed, diluted in 1 mL hexane (RMaia) and analyzed by Gas Chromatography with Flame Ionization Detector (GC-FID) in a Shimadzu CG-2010 apparatus, with SP™-2560 Supelco capillary column (100 m × 0.25 mm × 0.2 μm) using the following chromatographic conditions: initial temperature 140 °C

for 5 min followed by heating up to 240 °C at 4 °C min^{-1}, remaining at this temperature for 5 min (total run time of 35 min); injector temperature: 260 °C; FID detector temperature: 260 °C; helium gas carrier (1.1 mL min^{-1}); split rate 1:10, injected volume 1 μL. The quantification was made by the external standard method. The oleic acid to methyl oleate conversion percentages were calculated through the area of each peak formed during the reactions under the different proposed conditions.

The reuse tests were carried out under the optimal reaction conditions established by experiments with fresh catalysts. Before being reused the catalysts were washed with hot water (approx. 60 °C) at a ratio of 1:30 and dried in an oven at 120 °C for 15 h. Three cycles of reactions were conducted. At the end of the reuse tests, the catalysts were dried in an oven at 120 °C for 15 h and characterized by FTIR.

3. Result and discussions

3.1. Characterization of catalysts

The result of the thermogravimetric analysis of LO showed two mass loss intervals: between 260–370 °C and 380–470 °C probably due to the loss of water molecules and impurities that were retained on the surface of the material. SLO presented mass loss intervals between 25 and 300 °C and between 800 and 1000 °C that can be attributed, respectively, to the water and volatile material loss and to the decomposition of the sulfate groups adsorbed on the surface of the solid during the sulfation stage (Corma et al., 1994).

DTA analysis of LO showed two endothermic peaks at 300 and 455 °C, that can characterize physical processes such as vaporization of water and/or some dehydration reactions. However, SLO catalyst presented endothermic peaks at approximately 100 and 940 °C, responding to the water loss by vaporization and the decomposition of sulfate groups, respectively (Bernal et al., 2002). HZSM-5 and SLO/HZSM-5 thermograms showed similar and stable profiles, with a small weight loss concerning water molecules.

According to SEM micrographs, LO had the smallest grain size, although SLO presented a variation in the form and in the size of its grains, being between 17 and 150 μm. HZSM-5 showed small grains and fractions of amorphous materials, characterized by a clear portion, indicating that this sample may contain extraframework alumina. In the sample SLO/HZSM-5, the lighter portion is either extraframework alumina or the group SO_4^{2-}/La_2O_3 on the structure of the material.

Specific surface areas for the studied catalysts obtained using BET method (S_{BET}) were: 2 and 0.2 m^2g^{-1} for LO and SLO, respectively (Table 1). It is observed that the sulfation of LO led to a decrease in specific surface area (S_{BET}). It was also observed that the incorporation of SLO group in the structure of HZSM-5 caused a decrease in specific surface area (S_{BET}) of SLO/HZSM-5 (Table 1). From these results it can be concluded that the calcination temperature and also the concentration of the sulfuric acid solution used in the La_2O_3 sulfation process might have caused negative effects in the S_{BET} values. These effects were also reported by Pereira et al. (2008), who observed that the increase of both calcination temperature and sulfuric acid concentration resulted in a decrease in specific surface area.

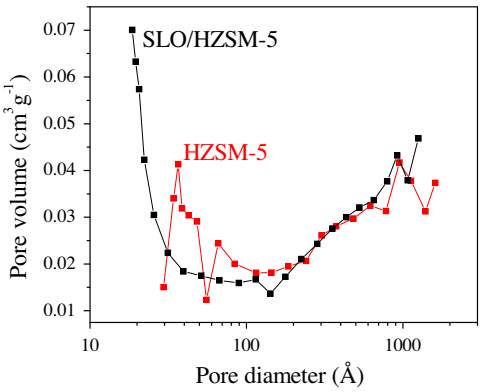

Fig. 1. Pores diameter distribution of HZSM-5 and SLO/HZSM-5.

Evaluating the results obtained for HZSM-5 and SLO/HZSM-5, it is observed that the incorporation of SO_4^{2-}/ La_2O_3 to HZSM-5 not only led to a decrease in S_{BET}, but also in all other parameters evaluated, indicating a partial obstruction of the pores of HZSM-5 by SLO (Table 1).

Fig. 1 shows the distribution of pores in HZSM-5 and SLO/HZSM-5 calculated by the BJH method. It can be seen that the pore distribution of HZSM-5 ranged from 35 to 2100 Å, while for SLO/HZSM-5 the distribution was 52–1200 Å . It is observed that pores with a diameter of 35–56 Å and greater than 1200 Å were not observed in the SLO/HZSM-5 sample, indicating probably that the SLO groups are blocking the pores of HZSM-5.

The LO FTIR spectrum presented a band around 3600 cm^{-1} that can be attributed to LaOH bonds (Tynjala and Pakkanen, 1996) and to adsorbed water molecules. However, the band found at 635 cm^{-1} can be attributed to the La–O bond. SLO presented absorption bands between 1285 and 1000 cm^{-1} that could be attributed to the sulfate group's vibration modes. The bands at 1285 and 1129 cm^{-1} are attributed to the asymmetrical and symmetrical S=O bond stretching, respectively. Furthermore, the bands found at 1000 and 820 cm^{-1} can be assigned to asymmetrical and symmetrical stretchings of the S=O bond, respectively (Noda et al., 2005; Almeida et al., 2008). The band found at 3400 cm^{-1} is the O–H bond vibration and also that of La-OH groups.

The bands due to hydroxyl groups of zeolites are the most important ones and are divided into terminals silanols (3740 cm^{-1}), hydroxyl groups at defect sites (3720 cm^{-1}), outside the crystal lattice OH (3680 cm^{-1}), the bridge OH as Al–Si–OH with the character Brønsted acid sites (3600–3650 cm^{-1}) and stretchings of OH of water molecules (3440 cm^{-1}). The bands at 1223 and 1092 cm^{-1} are attributed to the symmetrical stretching of Si–O–Si. The band present in the region of 803 cm^{-1} refers to the symmetrical stretching Si–O–Si framework in the structure. The band at 1630 cm^{-1} corresponds to the adsorbed water molecules. The SLO/HZSM-5 sample showed a decrease in the intensity of the band 3646 cm^{-1}, which can be related to the interaction between the zeolite and lanthanum, as observed by Moreira et al.

Table 1
Textural analysis of the catalysts.

Catalyst	Area (m^2 g^{-1})			Volume (cm^3 g^{-1})			D_p (A)
	BET	Micropores	External	Total	BJH	Micropores	
HZSM-5	286	267	19	0.2	0.07	0.1	25
SLO/HZSM-5	217	200	17	0.1	0.05	0.09	25

(2010). They have attributed this effect to hydroxyl groups associated to rare earth cations, which can be related to the presence of La^{3+} species oligomerized with the zeolitic material. The same bands observed for HZSM-5 in the region 1223–803 cm^{-1} were found in the spectrum of SLO/HZSM-5. The bands in this region are characteristic of SO_4^{2-} groups which are assigned to the vibration modes of sulfate groups (Noda et al., 2005; Almeida et al., 2008).

Lewis and Brønsted acid sites were identified through the analysis of FTIR spectra, using pyridine as a probe molecule. This molecule generated species with characteristic vibrations that were correlated to Lewis and Brønsted acid sites. The Brønsted sites can be found between 1630 and 1540 cm^{-1} and, Lewis sites in the 1455–1450 cm^{-1} region. The band found in the region of 1490 cm^{-1} can be attributed to Brønsted sites as well as Lewis (Tynjala and Pakkanen, 1996).

For LO, only Lewis acid sites related bands were found and a single band (1490 cm^{-1}) that can be attributed to Brønsted and Lewis sites. The Lewis sites found are weak, because, above 250 °C they were no longer observed. For SLO the presence of Brønsted acid sites is observed (1640, 1545 and 1470 cm^{-1}) and Lewis (1610, 1470 and 1445 cm^{-1}). The sample presents strong and weak Brønsted sites and weak Lewis sites.

When speaking of the acidity of sulfated oxides, it should be taken into consideration that the sulfate group is covalently bonded to the metal, leading to alterations in its structure, which is then reflected in their vibrational spectra. In the sulfated oxides many Brønsted acid sites can exist. The superacidity of these materials can be attributed to Brønsted sites created or already existent on the surface of these materials, whose acidity is increased by the presence of neighboring Lewis acid sites. The force of those Lewis acid sites is due to an inductor effect exercised by the sulfate group

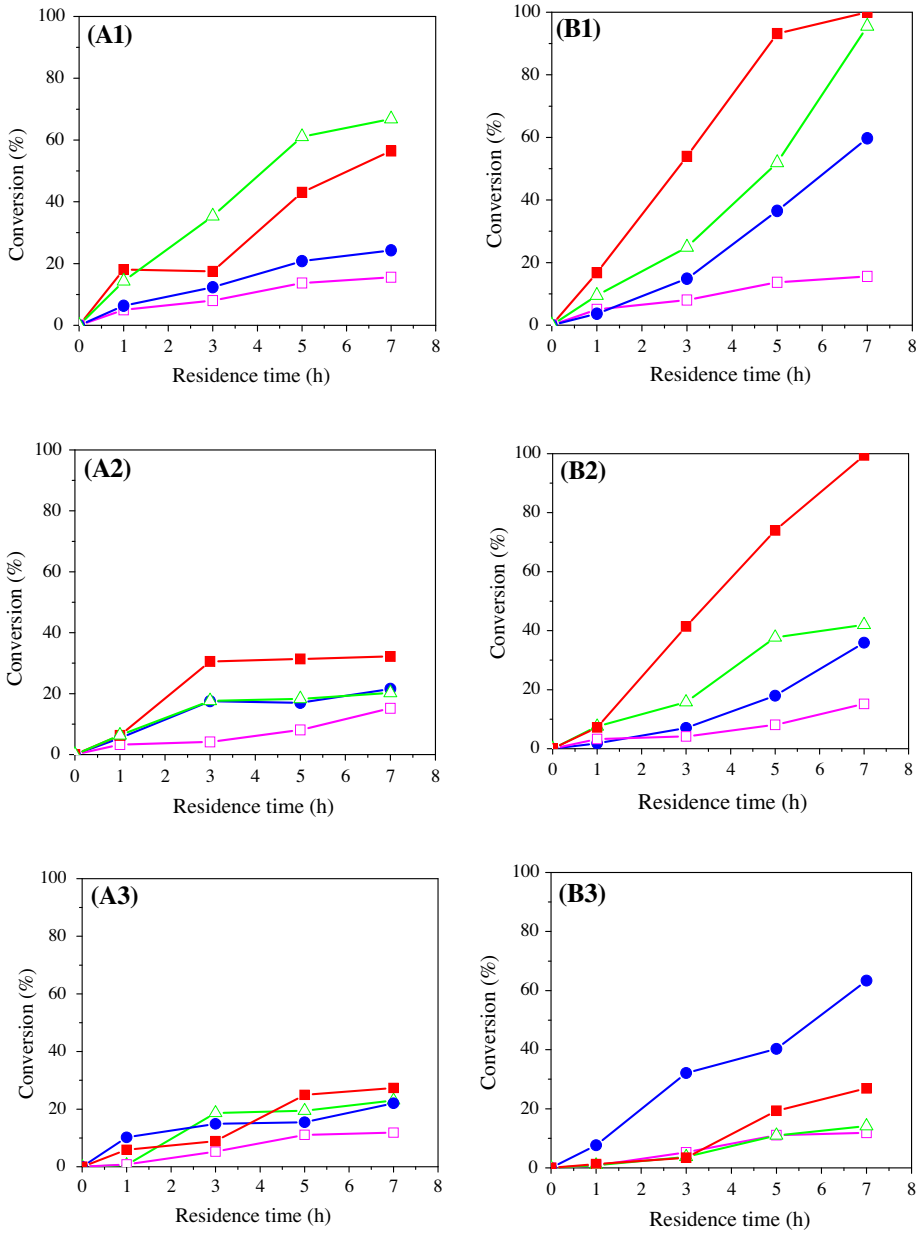

Fig. 2. Influence of amount of catalyst (LO (A), SLO (B)) and the m_{OA}/m_{MeOH} ratio (1:5 (1); 1:10 (2); 1:20 (3)) on the conversion of oleic acid to methyl oleate at 100 °C. Without catalyst (□), 5% (●), 10% (△) e 20% (■).

on the metallic cation, that becomes more electron deficient (Noda et al., 2005; Almeida et al., 2008).

HZSM-5 presented a shoulder in the region from 1660 to 1600 cm^{-1} comprising Lewis and Brønsted acid sites. A band was also observed in 1540 cm^{-1} (Brønsted sites) and 1490 cm^{-1} (Lewis and Brønsted sites). The desorption curves of HZSM-5 showed that there are strong Brønsted acid sites. The spectrum profile observed for SLO/HZSM-5 is very similar to the one obtained for HZSM-5. However stronger sites were observed, indicating that the deposition SO_4^{2-}/La_2O_3 on HZSM-5 leads to changes in the acid properties of the final catalyst.

According to Shu et al. (2007), a lanthanium atom could replace an aluminum atom in the bridging hydroxyl groups, and this isomorphic substitution would result in the formation of new acid sites similar to Brønsted acid sites. Furthermore, the exchange that occurs between La^{3+} and zeolites may result in the formation of metal cations hydrates $[La(OH)]^{2+}$ due to electrostatic field of the metal cation. The division of water molecules will occur to form $La(OH)^{2+}$, and a new Brønsted acid site will also be formed from this process.

3.2. Determination of optimum reaction conditions

3.2.1. Evaluation of the optimal amount of catalyst and best oleic acid/methanol mass ratio

Figs. 2 and 3 show the influence of the catalyst percentage and the oleic acid/methanol mass ratio (m_{OA}/m_{MeOH} ratio) on the conversion of oleic acid to methyl oleate. In the data presented in Fig. 2A and B, it is observed that for LO as well as SLO, the m_{OA}/m_{MeOH} ratio at which the best results were obtained was 1:5 (Fig. 2A1 and B1) for all variations of amount of catalyst tested. The influence of m_{OA}/m_{MeOH} ratio was more accentuated when 10% and 20% of catalyst were used. It was observed, according to the data presented, that there was an increase in the conversion with the decrease of m_{OA}/m_{MeOH} ratio.

In the data presented in Fig. 3A and B, it is observed that, for HZSM-5, the molar ratio of 1:20 (Fig. 3A3) gave the highest conversions at 10% and 20% catalyst in the reaction (conversion close to 80%). As for the SLO/HZSM-5 (Fig. 3B1), the best results were obtained using a ratio of 1:5 with 10% of catalyst (100% conversion).

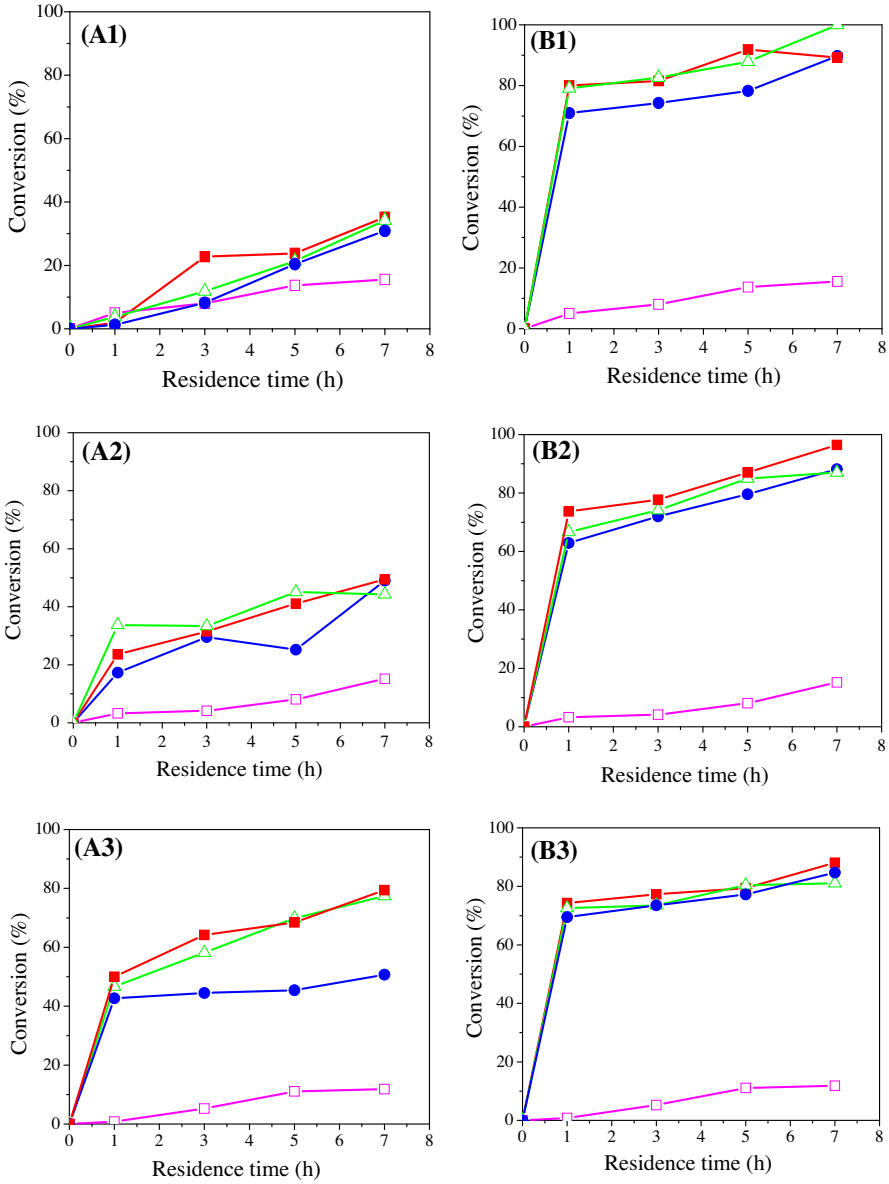

Fig. 3. Influence of amount of catalyst (HZSM-5 (A), SLO/HZSM-5 (B)) and the m_{OA}/m_{MeOH} ratio (1:5 (1); 1:10 (2); 1:20 (3)) on the conversion of oleic acid to methyl oleate at 100 °C. Without catalyst (□), 5% (●), 10% (△) e 20% (■).

Analyzing the variation of the oleic acid/methanol ratio, the best ratio for HZSM-5 was 1:20. The reason for this may be Le Chatelier's principle. When the alcohol concentration increases, the tendency of equilibrium, in principle, would be to move in favor of products, increasing thereby the yield of the ester formed. In addition, the increase in the concentration of alcohol may be promoting a reduction in the viscosity of the mixture, leading to better mixing of reagents and catalyst and to an improvement in the rate of mass transfer, resulting thus in a higher conversion. As for the other catalysts, the best ratio was 1:5, contrary to the theory proposed above, but this may have occurred because increasing the amount of alcohol may be inhibiting the reaction of esterification of oleic acid, probably due to a competition between methanol and oleic acid for active sites of the catalyst.

In most of the results appraised it can be observed that as the amount of catalyst increased, the amount methyl oleate formed also increased. This can be explained, because increasing the amount of catalyst in the reaction environment consequently increased the number of active sites necessary for the reaction to occur (Lam et al., 2009). It is also noticed by the results that there is a limit at which the variation of the catalyst amount causes an insignificant increase in the conversion. In other words, starting from that amount, to increase the catalyst mass in the reaction medium would not bring significant variations in the conversions.

3.2.2. Influence of temperature on the esterification reaction

After determining the best m_{OA}/m_{MeOH} ratio and amount of catalyst conditions to obtain the highest oleic acid conversion to methyl oleate, the effect of temperature on the reaction was studied. Fig. 4 presents the results. For LO (Fig. 4A) catalyst, the highest conversion was obtained when working at 100 °C and, there was practically no reaction at 50 °C. We observed that for SLO (Fig. 4B) the conversion at 100 °C was close to 100% and at 75 °C, around 80%. For HZSM-5 (Fig. 4C), at 75 and 50 °C, virtually there was no reaction. For SLO/HZSM-5 (Fig. 4D), the conversion at 75 °C was close to 80%. According to the results presented, we can observe that the sulfated material showed high activity at 75 °C. Therefore, the temperature increase resulted in higher conversions, which is line with kinetic (Arrhenius) and thermodynamic theory. According to Ramesh et al. (2010), due to the fact that the esterification reaction is endothermic, a higher yield will be reached when higher temperatures are used.

Yan et al. (2009b) proposed an esterification reaction mechanism. According to this mechanism, the esterification reaction occurs between the fatty acid adsorbed on the catalyst surface and the free alcohol, and the interaction of the fatty acid carbonyl oxygen with the acid sites (L+) of the catalyst will lead to the formation of the carbocation. The nucleophilic attack of the alcohol on the carbocation will then produce a tetrahedral intermediate and this intermediate will eliminate a water molecule to form the ester molecule. In this reaction, as already mentioned, the excess of alcohol provides higher ester yield.

According to the mechanism proposed by Yan et al. (2009b) and the obtained results, it can be suggested that the reaction is processed with methanol in gas phase (methanol ebullition temperature is 65 °C). Thus, on increasing the 50 °C temperature to 75 °C, the increase of the conversion can be attributed, mainly, to the methanol phase change. However, when the temperature is increased from 75 to100 °C, the increase of the conversion can be attributed to the kinetic and thermodynamic effects.

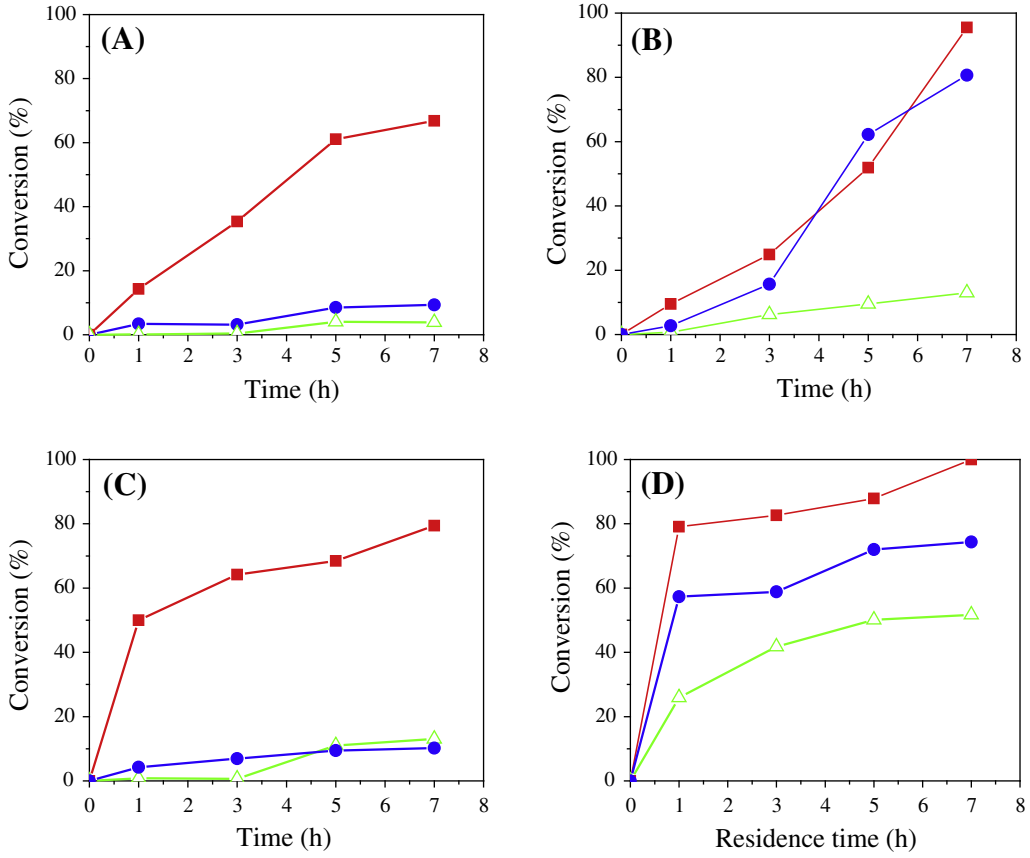

Fig. 4. Influence of temperature (50 °C (△), 75 °C (●) e 100 °C (■)) on the activity of LO (A), SLO (B), HZSM-5 (C) and SLO/HZSM-5 (D).

Table 2
Arrhenius parameters for the reaction of esterification of oleic acid and methanol.

Catalyst	E_a (kJ mol^{-1})	R
LO	55.77	0.9482
SLO	45.18	0.9919
HZSM-5	56.78	0.9507
SLO/HZSM-5	43.66	0.9655
Without catalyst	68.37	0.9963

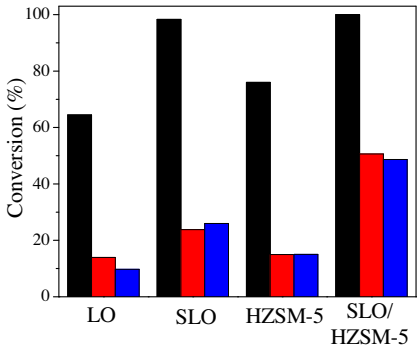

Fig. 5. Recyclability of catalysts (1st use (■), 2nd use (■) and 3rd use (■)).

3.3. Determination of system activation energy

The activation energies (E_a) were determined using the equation of Arrhenius (Eq. (1)). The analyses were made according to the first order kinetic model (Yan et al., 2009a) and the results are in Table 2.

$$\ln k = \ln A - \frac{E_a}{RT} \quad (1)$$

where k = rate constant; A = Arrhenius factor; E_a = process activation energy; R = 8.314 J mol^{-1}K^{-1} and T = temperature in K.

The activation energies obtained are in agreement with the conversion results, in other words, the lowest value was found for the most active catalyst. E_a of the non-catalyzed reaction was also determined and it was observed that the value found is superior to the values found for the catalyzed reactions.

3.4. Reuse tests of catalysts

Fig. 5 presents the reusability of catalyst through three consecutive cycles. The tests were performed in optimized conditions: 100 °C, 7 h, 10% catalyst, m_{OA}/m_{MeOH} ratio 1:5 (except for ZSM-5 that was 1:20). All catalysts deactivated after the first cycle, but the deactivation of SLO/HZSM-5 was smaller. After the second cycle the deactivation was not significant, except for LO.

The FTIR spectra of methyl oleate and the fresh catalyst and after the third reuse were recorded. In the reused catalyst spectrum, the appearance of bands at 2926 and 2854 cm^{-1}, corresponding respectively to vibration of symmetrical and asymmetrical stretching of the C–H bond of methyl group and to vibrations of asymmetric and symmetric stretching of the C–H bond of the methylene group suggests the presence of organic residues not removed from the structure of the materials after washing the solids. The band around 1740 cm^{-1} can be attributed to ester carbonyl functional group and the bands at 1238 and 1163 to the stretching vibrational of CO group (Yan et al., 2009).

These results show that the deactivation of the catalysts can be attributed to the impregnation of the ester in the active sites. Nevertheless, the deactivation of the catalysts can also be attributed to changes in the structure of the catalysts during the reaction or the washing and drying process.

4. Conclusion

The catalysts were shown to be efficient and promising for the esterification of oleic acid with methanol. The sulfation process led to a decrease of the specific surface area of the catalysts and caused the formation of strong Brønsted acid sites.

m_{OA}/m_{MeOH} ratio equals to 1:5 and 10% of catalyst led to the best results for LO, SLO and SLO/HZSM-5. At 100 °C the best conversions were obtained, while at 50 °C the yields were very inferior, suggesting that the physical state of the methanol can be an important factor. All catalysts deactivated, but the deactivation of SLO/HZSM-5 was smaller.

Acknowledgements

To CAPQ/UFLA for the chromatographic analysis, to CNPq for financial support and scholarship, to NUCAT/PEQ/COPPE, for BET analysis and to the Instituto Nacional de Tecnologia, for performing the FTIR-Py analysis.

References

Almeida, R.M., Noda, L.K., Gonçalves, N.S., Meneghetti, S.M.P., Meneghetti, M.R., 2008. Transesterification reaction of vegetable oils, using superacid sulfated TiO_2-base catalysts. Appl. Catal. A 347, 100–105.
Aranda, D.A.G., Gonçalves, J.A., Peres, J.S., Ramos, A.L.D., Melo Jr., C.A.R.O., Antunes, A.C., Furtado, N.C., Taft, C.A., 2009. The use of acids, niobium oxide, and zeolite catalysts for esterification reactions. J. Phys. Org. Chem. 22, 709.
Bernal, C., Couto, A.B., Breviglieri, S.T., Cavalheiro, É.T.G., 2002. Influence of some experimental parameters on the results of differential scanning calorimetry – DSC. Quim. Nova 25, 849–855.
Birla, A., Singh, B., Upadhyay, S.N., Sharma, Y.C., 2012. Kinetics studies of synthesis of biodiesel from waste frying oil using a heterogeneous catalyst derived from snail shell. Bioresour. Technol. 106, 95–100.
Cassinelli, W.H., Feio, L.S.F., Araújo, J.C.S., Hori, C.E., Noronha, F.B., Marques, C.M.P., Bueno, J.M.C., 2008. Effect of CeO_2 and La_2O_3 on the activity of CeO_2–La_2O_3/Al_2O_3 supported Pd catalysts for steam reforming of methane. Catal. Lett. 120, 86–94.
Chang, B., Fu, J., Tian, Y., Dong, X., 2012. Mesoporous solid acid catalysts of sulfated zirconia/SBA-15 derived from a vapor-induced hydrolysis route. Appl. Catal. A 437–438, 149–154.
Chantras, A., Phlernjai, N., Goodwin Jr., J.G., 2011. Kinetics of hydrotalcite catalyzed transesterification of tricaprylin and methanol for biodiesel synthesis. Chem. Eng. J. 168, 333–340.
Chung, K.H., Chang, D., Park, B., 2008. Removal of free fatty acid in waste frying oil by esterification with methanol on zeolite catalysts. Bioresour. Technol. 99, 7438–7443.
Chung, K.H., Park, B.G., 2009. Esterification of oleic acid in soybean oil on zeolite catalysts with different acidity. J. Ind. Eng. Chem. 15, 388–392.
Corma, A., Fornes, V., Juan-Rajadell, M.I., López Nieto, J.M., 1994. Influence of preparation conditions on the structure and catalytic properties of SO_4^{2-}/ZrO_2 superacid catalysts. Appl. Catal. A 116, 151–163.
Costa, A.A., Braga, P.R.S., Macedo, J.L., Dias, J.A., Dias, S.C.L., 2012. Structural effects of WO_3 incorporation on USY zeolite and application to free fatty acids esterification. Microporous Mesoporous Mater. 147, 142–148.
Encinar, J.M., Sánchez, N., Martínez, G., García, L., 2011. Study of biodiesel production from animal fats with high free fatty acid content. Bioresour. Technol. 102, 10907–10914.
Fatsikosta, A.N., Kondarides, D.I., Verykios, X.E., 2002. Production of hydrogen for fuel cells by reformation of biomass-derived ethanol. Catal. Today 75, 145–155.
Furuta, S., Matsuhashi, H., Arata, K., 2004. Biodiesel fuel production with solid superacid catalysis in fixed bed reactor under atmospheric pressure. Catal. Commun. 5, 721–723.
Kafuku, G., Lam, M.K., Kansedo, J., Lee, K.T., Mbarawa, M., 2010. Heterogeneous catalyzed biodiesel production from Moringa oleifera oil. Fuel Process. Technol. 91, 1525–1529.
Kim, M., DiMaggio, C., Salley, S.O., Simon Ng, K.Y., 2012. A new generation of zirconia supported metal oxide catalysts for converting low grade renewable feedstocks to biodiesel. Bioresour. Technol. 118, 37–42.
Kirumakki, S.R., Nagaraju, N., Chary, K.V.R., 2006. Esterification of alcohols with acetic acid over zeolites Hβ, HY and HZSM-5. Appl. Catal. A 299, 185–192.
Lam, M.K., Lee, K.T., Mohamed, A.R., 2009. Sulfated tin oxide as solid superacid catalyst for transesterification of waste cooking oil: an optimization study. Appl. Catal. B 93, 134–139.

Li, Y., Zhang, X.D., Sun, L., Zhang, J., Xu, H.P., 2010. Fatty acid methyl ester synthesis catalyzed by solid superacid catalyst $SO_4^{2-}/ZrO_2–TiO_2/La^{3+}$. Appl. Energy 87, 156–159.

Lima, S.M., Silva, A.M., Costa, L.O.O., Assaf, J.M., Jacobs, G., Davis, B.H., Mattos, L.V., Noronha, F.B., 2010. Evaluation of the performance of Ni/La_2O_3 catalyst prepared from $LaNiO_3$ perovskite-type oxides for the production of hydrogen through steam reforming and oxidative steam reforming of ethanol. Appl. Catal. A 377, 181–190.

Marchetti, J.M., Errazu, A.F., 2008. Esterification of free fatty acids using sulfuric acid as catalyst in the presence of triglycerides. Biomass Bioenergy 32, 892–895.

Moreira, C.R., Homs, N., Fierro, J.L.G., Pereira, M.M., Piscina, P.R., 2010. HUSY zeolite modified by lanthanum: effect of lanthanum introduction as a vanadium trap. Microporous Mesoporous Mater. 133, 75–81.

Noda, L.K., Almeida, R.M., Probst, L.F.D., Gonçalves, N.S., 2005. Characterization of sulfated TiO_2 prepared by the sol–gel method and its catalytic activity in the *n*-hexane isomerization reaction. J. Mol. Catal. A Chem. 225, 39–46.

Patel, A., Narkhede, N., 2012. 12-Tungstophosphoric acid anchored to zeolite Hβ: synthesis, characterization, and biodiesel production by esterification of oleic acid with methanol. Energy Fuels 26, 6025–6032.

Pereira, A.L.C., Marchetti, S.G., Albornoz, A., Oportus, M., Reyes, P., Rangel, M.C., 2008. Effect of iron on the properties of sulfated zirconia. Appl. Catal. A 334, 187–198.

Ramesh, S., Prakash, B.S., Bhat, J.Y.S., 2010. Enhancing Brønsted acid site activity of ion exchanged montmorillonite by microwave irradiation for ester synthesis. Appl. Clay Sci. 48, 159-153.

Russbueldt, B.M.E., Hoelderich, W.F., 2010. New rare earth oxide catalysts for the transesterification of triglycerides with methanol resulting in biodiesel and pure glycerol. J. Catal. 271, 290–304.

Satyarthi, J.K., Radhakrishnan, S., Srinivas, D., 2011. Factors influencing the kinetics of esterification of fatty acids over solid acid catalysts. Energy Fuels 25, 4106–4112.

Selvabala, V.S., Selvaraj, D.K., Kalimuthu, J., Periyaraman, P.M., Subramanian, S., 2011. Two-step biodiesel production from *Calophyllum inophyllum* oil: optimization of modified b-zeolite catalyzed pre-treatment. Bioresour. Technol 102, 1066–1072.

Semwal, S., Arora, A.K., Badoni, R.P., Tuli, D.K., 2011. Biodiesel production using heterogeneous catalysts. Bioresour. Technol. 102, 2151–2161.

Shu, Q., Yang, B., Yuan, H., Qing, S., Zhu, G., 2007. Synthesis of biodiesel from soybean oil and methanol catalyzed by zeolite beta modified with La^{3+}. Catal. Commun. 8, 2159–2165.

Tynjala, P., Pakkanen, T.T., 1996. Acidic properties of ZSM-5 zeolite modified with Ba^{2+}, Al^{3+} and La^{3+} ion-exchange. J. Mol. Catal. A Chem. 110, 153–161.

Yan, S., Kim, M., Salley, S.O., Simon, K.Y., 2009a. Oil transesterification over calcium oxides modified with lanthanum. Appl. Catal. A 360, 163–170.

Yan, S., Salley, S.O., Ng, K.Y.S., 2009b. Simultaneous transesterification and esterification of unrefined or waste oils over $ZnO–La_2O_3$ catalysts. Appl. Catal. A 353, 203–212.

Yin, P., Chen, L., Wang, Z., Qu, R., Liu, X., Ren, S., 2012. Production of biodiesel by esterification of oleic acid with ethanol over organophosphonic acid-functionalized silica. Bioresour. Technol. 110, 258–263.